Diabetes, Metabolic Syndrome and Obesity

Dovepress
Taylor & Francis Group

Open Access Full Text Article

ORIGINAL RESEARCH

Effect of Lifestyle Intervention on the Mobilization of Fat Depots and Organ Iron Deposition in Individuals with Obesity: A Prospective Study

Hong Liu[1,2,*], Junhong Duan[3,*], Gaopeng Guan[1], Pengfei Rong[3], Ping Jin[1,4]

[1]Department of Endocrinology, The Third Xiangya Hospital of Central South University, Changsha, Hunan, People's Republic of China; [2]Department of Nutrition, The Third Xiangya Hospital of Central South University, Changsha, Hunan, People's Republic of China; [3]Department of Radiology, The Third Xiangya Hospital of Central South University, Changsha, Hunan, People's Republic of China; [4]Key Technologies and Application Evaluation of Intelligent Assisted Diagnosis and Treatment in Hunan Provincial Engineering Research Center, Changsha, Hunan, People's Republic of China

*These authors contributed equally to this work

Correspondence: Ping Jin, Department of Endocrinology, The Third Xiangya Hospital, Central South University, 138 Tongzipo St, Changsha, Hunan, 410013, People's Republic of China, Email ping.jin06@csu.edu.cn

Purpose: To investigate how lifestyle interventions alter fat distribution and organ-specific iron deposition in individuals with obesity, and whether these changes can serve as indicators of glycemic remission in obese patients with dysglycemia.

Methods: This prospective study included individuals with obesity who participated in a 6-month lifestyle intervention, which comprised a caloric-restricted balanced diet and an exercise regimen. Ultimately, 104 participants completed the follow-up phase. Magnetic resonance imaging (MRI) was utilized to monitor the dynamics of fat mobilization and organ iron deposition at baseline and 6-month follow-up. Correlation analysis, logistic regression, and receiver operating characteristic (ROC) curve analysis were employed to examine the relationships between regional fat distribution, organ iron deposition, and glycemic improvement.

Results: Initially, the 104 participants were divided into three categories: normal glucose regulation (NGR, n=41), prediabetes (n=23), and type 2 diabetes mellitus (T2DM, n=40). After a 6-month lifestyle change, the number of patients with T2DM and prediabetes decreased, and those with NGR increased. There were also notable decreases in liver and pancreatic fat, as well as visceral and subcutaneous fat, with the largest decrease in liver fat (−43.2%) among obese participants. There were also reductions in liver and pancreatic iron deposition after intervention. ROC curve analysis revealed that the change in liver fat was the best indicator of diabetes remission among obese participants, with an area under the curve of 0.819 (95% confidence interval [CI]: 0.681–0.957). Notably, liver fat reduction ≥38.8% predicted diabetes remission (OR=2.5, 95% CI:1.59–5.60) in individuals with obesity.

Conclusion: Lifestyle intervention can effectively reduce ectopic fat and iron overload in individuals with obesity. The extent of hepatic fat mobilization has emerged as the most significant indicator of diabetes remission in individuals with obesity, potentially serving as a pivotal focus for future therapeutic interventions.

Keywords: obesity, type 2 diabetes, MRI, fat mobilization, iron deposition, lifestyle intervention

Introduction

Obesity has become a global epidemic, affecting over one billion individuals worldwide.[1] Obesity, particularly central obesity, has been firmly established as a major risk factor for metabolic disorders such as type 2 diabetes mellitus (T2DM).[2] A key pathological feature of central obesity is body fat redistribution and ectopic fat deposition.[3] This ectopic fat deposition in non-adipose tissues, particularly the liver and pancreas, differs fundamentally from that in visceral fat (eg, mesenteric and perirenal fat) and subcutaneous fat (defined as fat stored beneath the skin).[2] Fat accumulation in both the liver and pancreas is associated with impaired glucose metabolism.[4] Emerging evidence suggests that in addition to fat accumulation, iron overload contributes to metabolic disorders.[5,6] Elevated serum ferritin predicts diabetes risk,[5,6] but its specificity is limited as an acute-phase reactant influenced by inflammation, liver disease, and insulin resistance.[7–9]

Received: 9 September 2025
Accepted: 3 November 2025
Published: 11 November 2025

The role of organ-specific iron deposition (eg, hepatic and pancreatic iron overload) in metabolic dysfunction is still unclear.

Traditional anthropometrics such as body mass index (BMI), waist circumference, or bioelectrical impedance analysis have significant limitations in assessing ectopic fat deposition. Magnetic resonance imaging (MRI), particularly the mDIXON technique, provides a noninvasive gold standard for quantifying both fat (via the proton density fat fraction, PDFF) and iron deposition (via R2*).[10] Importantly, the MRI-PDFF assessment is highly concordant with liver biopsy assessment regarding changes in liver histology.[11] Existing studies have examined fat deposition within individual organs separately,[12,13] failing to address the combined metabolic effects of multisite fat distribution and organ-specific iron deposition. This study utilizes MRI-based multiorgan (liver, pancreas, visceral and subcutaneous adipose tissue) and multiparametric (fat-iron) quantitative assessments to comprehensively evaluate the relationships among region-specific ectopic fat deposition, organ-specific iron accumulation, and glucose metabolism in individuals with obesity. Previous studies have demonstrated that a 6-month lifestyle intervention period can induce measurable changes in visceral and ectopic fat depots, as well as improvements in glucose metabolism.[14–17] Therefore, in our study, all obese patients underwent a 6-month lifestyle intervention (including a caloric-restricted balanced diet and exercise intervention). We performed MRI-based quantification of the changes in fat and iron contents across key organs (liver, pancreas, visceral and subcutaneous adipose tissue) after intervention and analyzed their relationships with improvements in glucose metabolism.

Materials and Methods

Study Design and Participants

Study Design

This prospective study enrolled 128 individuals with obesity (68 males, 60 females; median age 40.8 years [interquartile range (IQR) 29.5–43.9]) from the Third Xiangya Hospital of Central South University, China between April 2024 and April 2025. The participants received lifestyle interventions exclusively, with no use of hypoglycemic medications throughout the study. Baseline and 6-month post-intervention assessments—including magnetic resonance imaging (MRI) and oral glucose tolerance tests (OGTTs)—were performed for all participants. The study was approved by the Institutional Review Board of the Third Xiangya Hospital (Approval No. Quick I 22218) and registered at ClinicalTrials.gov (NCT06441409, https://register.clinicaltrials.gov/prs/beta/records) in April 2024. All participants provided written informed consent. This study adheres to the Consolidated Standards of Reporting Trials (CONSORT).[18]

Inclusion and Exclusion Criteria

The participants were required to meet all the following inclusion criteria: (1) aged 18–70 years; (2) BMI ≥28 kg/m^2; (3) capacity to complete the protocol requirements; and (4) commitment to a 6-month lifestyle intervention. Key exclusions included the following: preexisting diabetes with glucose-lowering therapy; diabetes complications or major systemic diseases; active malignancy; acute/chronic infections; hemochromatosis; hepatitis (drug-induced/autoimmune/viral); unexplained transaminase elevation (>2×ULN); pancreatic disorders; iron deficiency anemia requiring supplementation; recent (6-month) blood donation/transfusion or cardiovascular events; excessive alcohol intake (>140 g/week [men], >70 g/week [women]); recent (3-month) weight-affecting medications or >5% weight fluctuation; and pregnancy/lactation.

Grouping of Participants

The 128 participants were stratified by an oral glucose tolerance test (OGTT) into normal glucose regulation (NGR, n=54), prediabetes (IFG and IGT, n=30), and type 2 diabetes (T2DM, n=44) groups. The criteria defining NGR were glycated hemoglobin (HbA1c) <5.7%, fasting plasma glucose (FPG) <110 mg/dl (6.1 mmol/L) and 2-h plasma glucose (PG) during the 75-g OGTT <140 mg/dl (7.8 mmol/L). The criteria defining prediabetes were an HbA1c level of 5.7–6.4%, an FPG level of 110 mg/dl (6.1 mmol/L) to 125 mg/dl (6.9 mmol/L) (IFG) or a 2-h PG during the 75-g OGTT 140 mg/dl (7.8 mmol/L) to 200 mg/dl (11.0 mmol/L) (IGT). The criteria for the diagnosis of diabetes were HbA1c ≥6.5%, FPG ≥126 mg/dl (≥7.0 mmol/L), 2-h PG ≥200 mg/dl (≥11.1 mmol/L) or a random PG ≥200 mg/dl (≥11.1 mmol/L) in an individual with classic symptoms of hyperglycemia or hyperglycemic crisis. The criterion for T2DM remission

after a 6-month lifestyle intervention was defined as an HbA1c level <6.5%. For prediabetes remission to NGR, the criteria require both OGTT results and HbA1c to fully meet the aforementioned NGR standards.

Research Methods

Lifestyle Intervention

Dietary Assessment

Dietary intake was evaluated in all participants with obesity via three consecutive 24-hour dietary recalls (including two weekdays and one weekend day) administered by certified dietitians according to the Chinese Health Industry Standard (WS/T 426.1–2013) at baseline and at the follow-up visits. Energy and nutrient intakes were calculated via the China Food Composition Table (Standard Edition, 6th version), with analysis focusing on macronutrient (carbohydrates, proteins, fats), dietary fiber, and iron intake.

Caloric-Restricted Balanced Diet

All participants received a 6-month individualized calorie-restricted balanced diet (CRD) designed by certified dietitians, with the resting energy expenditure measured via indirect calorimetry (COSMED C00600-01-11, USA) and daily energy intake set at 500 kcal below the estimated total energy expenditure (calculated via physical activity levels). The CRD provided 45–55% carbohydrates from low-glycemic index sources (whole grains/legumes), 15–20% protein from high-quality sources (lean meat/fish/eggs/soy/dairy), and 20–30% fat predominantly from unsaturated fats with restricted trans/saturated fats.

Exercise Intervention

All enrolled individuals with obesity underwent a 6-month structured exercise program consisting of (1) ≥150 minutes/week of moderate-intensity aerobic exercise (eg, brisk walking, cycling, swimming) and (2) ≥2 sessions/week of whole-body resistance training targeting major muscle groups (eg, squats, bench press, rowing), with 3 sets of 8–6 repetitions per session.

Implementation Protocol

The participants joined WeChat groups (≤30 members/group) supervised by 1–2 dietitians for daily meal photo monitoring, with monthly follow-ups, including anthropometric measurements (weight and waist–hip circumference), body composition analysis via bioelectrical impedance analysis (BIA), and individualized diet plan adjustments on the basis of progress tracking. Patients missing scheduled monthly visits will receive phone or WeChat reminders. Those failing to attend the 6-month final visit despite reminders and still absent within 1 week will be excluded from final analysis.

Biochemical Indicators

Demographic and anthropometric data (age, sex, height, weight, body mass index [BMI], waist–hip circumference, waist–hip ratio [WHR]), exercise habits, and current medications were extracted from electronic medical records, with 6-month changes denoted as Δweight, ΔBMI, and ΔWHR. Laboratory analyses included (1) liver/kidney function, triglyceride (TG), total cholesterol (TC), and ferritin levels measured by an automated biochemistry analyzer (Hitachi 7600, Japan); (2) HbA1c and OGTT (0,1,2-h glucose) via the enzymatic electrode method (Arkray GA-1172); and (3) insulin levels measured via electrochemiluminescence (Roche 601).

Calculation Formulas

Homeostasis model assessment of insulin resistance (HOMA-IR)[19] = (fasting plasma glucose [FPG] × fasting insulin)/22.5; HOMA of β-cell function (HOMA-β)[19] = 20 × fasting insulin/(FPG - 3.5); insulin sensitivity index (ISI)[19] = 10,000/(FPG × fasting insulin × 2-h glucose × 2-h insulin)$^{0.5}$; triglyceride–glucose index (TyG)[19] = Ln[fasting TG (mg/dL) × FPG (mg/dL)/2] (FPG/insulin units: mmol/L/μU/mL). Six-month changes were recorded as ΔTG, ΔTC, ΔHOMA-IR, ΔHOMA-β, and ΔISI.

https://doi.org/10.2147/DMSO.S564591

Magnetic Resonance Imaging (MRI)

All participants underwent fasting MRI scans at baseline and after the 6-month intervention via a 3.0T system (Philips INGENIA ELITION X, Netherlands) with multiecho Dixon sequences by a professional radiologist with 9 years of experience. The hepatic fat content [proton density fat fraction (PDFF), %] and iron deposition (iron/s) were derived from eight 100-mm^2 regions of interest (ROIs) in the right lobe (excluding major vessels/bile ducts). Hepatic steatosis was defined as a PDFF ≥5.0%.[20] The pancreatic fat content (PDFF,%) and iron deposition (iron,/s) were averaged from three 100 mm^2 ROIs (head/body/tail). The abdominal subcutaneous fat area (SFA) and visceral fat area (VFA, cm^2) at the L3 vertebra level were analyzed via Slice O matic software on T2-weighted images. Changes (Δ) and percentage changes (Δ%) were calculated as follows: Δ = baseline - follow-up; Δ% = (Δ/baseline)×100.

Outcome Measurements

The primary outcome of the study was the changes of site-specific fat and organ-specific iron deposition in individuals with obesity defined by MRI, calculated as (initial measurement − follow-up measurement) / (initial measurement) × 100 and predefined to be assessed at 6-month follow-up. The secondary outcome of the study was to investigate whether these changes can serve as indicators of glycemic remission in obese patients with dysglycemia.

Sample Size

The sample size was calculated based on the following assumptions: (1) a two-sided significance level of 0.05, (2) a statistical power of at least 90%, and (3) a priori hypothesis that lifestyle intervention would preferentially mobilize hepatic fat, followed by pancreatic fat, VAT, and SAT. Based on these assumptions, a minimum of 89 participants was required for the final analysis. Sample size estimation was performed using PASS software, version 22 (NCSS, LLC). To account for an anticipated dropout rate of 30%, the initial number of enrolled participants was set at 128 to ensure that the final achieved sample size would meet the study requirements.

Statistical Analysis

Data were analyzed via R 3.5.3 and SPSS 27.0. The categorical data are presented as n(%). Normality was assessed via the Shapiro–Wilk normality test, and homogeneity of variance was assessed via Levene's test. Normally distributed continuous variables are presented as the means ± SDs. Nonnormally distributed data are presented as medians (*Q1–Q3*). Chi-square tests (χ^2-tests) were used to compare categorical data. Independent t tests or Mann–Whitney *U*-tests were used to compare continuous variables between participants who completed follow-up and those who were lost to follow-up. A paired *t* test or Wilcoxon signed-rank test was used to compare continuous variables between baseline and the 6-month follow-up. Analysis of variance (ANOVA) or the Kruskal–Wallis test was used to compare continuous variables among the NGR, prediabetes, and T2DM groups. Pairwise comparisons among the three groups were performed with post hoc Bonferroni correction. A Sankey diagram was used to visualize changes in glucose metabolism types from baseline to the 6-month follow-up. Pearson correlation analysis or Spearman's rank correlation was used to assess the relationships between changes in hepatic and pancreatic fat or iron content, body composition and anthropometric measures, and insulin sensitivity or resistance indices.

Multinomial logistic regression analyses with multivariable adjustment were conducted to assess the independent associations of potential indicators with prediabetes and T2DM. Additionally, binary multivariable logistic regression was employed to assess the independent associations of potential indicators with two distinct binary outcomes: diabetes remission and the reversal of prediabetes to NGR. For continuous variables with potential prognostic value, optimal cutoffs were determined via receiver operating characteristic (ROC) curve analysis, and these continuous variables were dichotomized on the basis of their respective optimal cutoffs. ROC curves were plotted to evaluate the ability of changes in these parameters (Δhepatic fat%, Δhepatic iron%, Δpancreatic fat%, and Δpancreatic iron%, ΔVFA%, ΔSFA%, ΔBMI%) to reflect T2DM remission and reversal of prediabetes to NGR in individuals with obesity.

Results

Study Flowchart

Among the 128 individuals with obesity at baseline, 24 individuals were lost to follow-up at the 1-, 2-, 3-, 4-, 5-, or 6-month visits, and a total of 104 individuals completed both the 6-month MRI and OGTT assessments (flow diagram in Figure 1). There was no significant difference in baseline characteristics between individuals who were lost to follow-up and those who completed follow-up (Supplementary Table 1). After 6-month lifestyle intervention, among the 104 participants, 41 individuals with NGR at baseline maintained NGR status. Among the 23 participants with prediabetes at baseline, 21 achieved NGR, whereas 2 remained prediabetic. Among the 40 participants with T2DM at baseline, 16 achieved NGR, 2 regressed to prediabetes, and 22 persisted with T2DM (sankey diagram in Figure 2).

Associations Between Regional Fat Content, Iron Deposition, and Glucose Metabolism at Baseline

At baseline, the 104 participants were stratified into NGR (n=41, 39.4%), prediabetes (n=23, 22.1%) and T2DM (n=40, 38.5%) groups. No significant differences in age, BMI, or WHR were observed among the groups (all $P > 0.05$). Compared with the NGR or prediabetes group, the T2DM group presented significantly greater ferritin, TyG index and HOMA-IR values but lower HOMA-β values (all $P < 0.05$). Additionally, SFA, VFA, hepatic and pancreatic fat, and pancreatic iron deposition were also elevated in the T2DM group compared with the NGR or prediabetes group (all $P < 0.05$) (Table 1 and Supplementary Table 2).

In individuals with obesity, hepatic fat content was positively correlated with HOMA-IR ($r = 0.49$, $P < 0.001$) and hepatic iron deposition ($r = 0.67$, $P < 0.001$) but negatively correlated with the ISI ($r = -0.54$, $P < 0.001$); pancreatic fat content was negatively correlated with HOMA-β ($r = -0.27$, $P < 0.001$) and positively correlated with pancreatic iron deposition ($r = 0.77$, $P < 0.001$). Hepatic iron deposition was positively associated with HOMA-IR ($r = 0.24$, $P = 0.002$) and negatively associated with the ISI ($r = -0.29$, $P < 0.001$), whereas pancreatic iron deposition was negatively correlated with HOMA-β ($r = -0.26$, $P = 0.001$).

Initially, we employed ordinal multinomial logistic regression to analyze independent risk factors for prediabetes and T2DM at baseline. However, as the parallel regression assumption was not satisfied, we ultimately adopted unordered multinomial logistic regression for the final analysis. The dependent variable comprised three glycemic status categories:

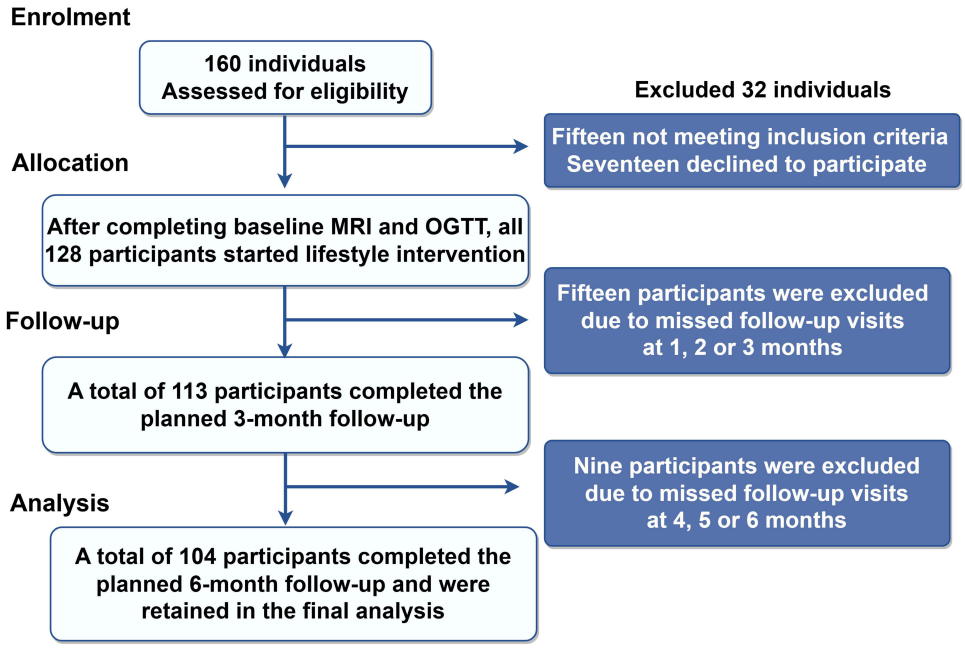

Figure 1 Flowchart of participant enrollment.

https://doi.org/10.2147/DMSO.S564591

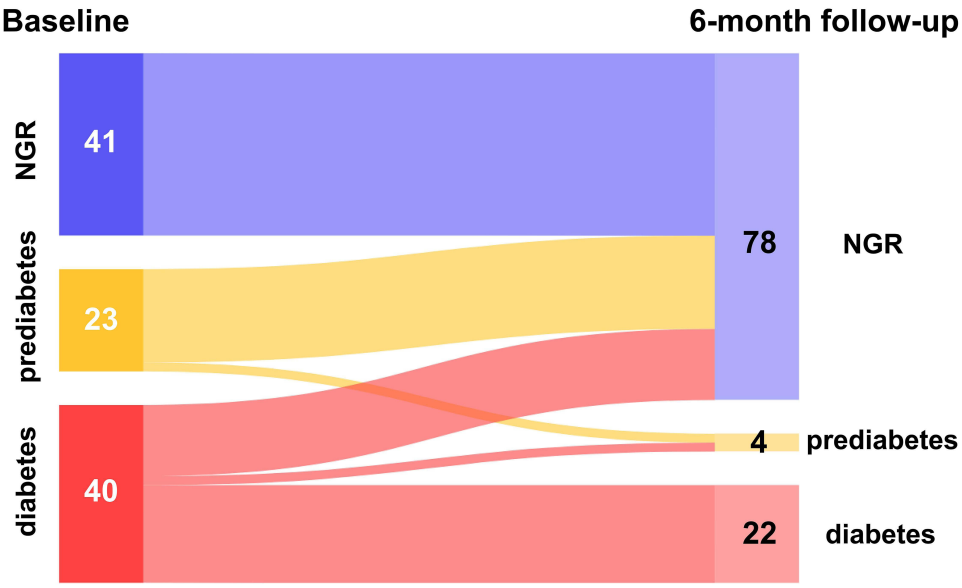

Figure 2 Transitions in glucose metabolism types from baseline to the 6-month follow-up.

normal glucose regulation (reference group), prediabetes, and T2DM. Independent variables included sex (categorical variable with males as the reference group), age, BMI, ferritin, hepatic fat content (categorical variable with ≥ 5% as the hepatic steatosis, <5% as the reference group), hepatic iron deposition, pancreatic fat content, pancreatic iron content, visceral fat area, and subcutaneous fat area. All independent variables except sex and hepatic fat content were continuous variables. We found that only hepatic fat content was identified as an independent risk factor for T2DM in individuals

Table 1 Clinical Characteristics of Obese Patients with Different Glycemic States

	NGR (n=41)	Prediabetes (n=23)	T2DM (n=40)	*P*
Age, years[a]	39.2 (28.1,42.2)	40.8(30.1,45.3)	42.7(30.2,45.4)	0.218
Male [b]	21 (51.2)	11 (47.8)	22(55.0)	0.939
BMI, kg/m^2 [a]	30.4 (28.3,33.4)	31.4(29.5,33.8)	31.0(28.4,32.4)	0.317
Waist hip ratio [c]	0.94±0.07	0.95±0.09	0.95±0.07	0.755
Triglycerides, mmol/L[a]	1.4(0.8,2.4)	2.1(1.3,2.6)	2.6(1.6,3.3)	<0.001
TC, mmol/L[a]	4.8(4.1,5.3)	5.2(4.8,5.8)	5.5(5.0,6.4)	<0.001
Ferritin, μg/L[a]	85(54,194)	110(68,218)	275(177,481)	<0.001
TyG index [c]	3.8±0.4	4.1±0.5	4.3±0.5	<0.001
HbA1c, % [a]	5.2 (5.0, 5.5)	6.0 (5.8, 6.3)	7.2 (7.0, 7.5)	<0.001
HOMA-IR [a]	4.3(3.4,5.7)	4.4(3.5,7.0)	6.3(4.5,10.4)	0.008
HOMA-β,% [a]	255(199,339)	170(80,261)	65(34,93)	<0.001
ISI [a]	43.4(31.2,61.5)	25.0(17.0,41.2)	23.1(17.0,37.6)	<0.001
SFA, cm^2 [a]	251(201,307)	211(171,331)	190(123,264)	0.002
VFA, cm^2 [a]	121(91,156)	145(99,189)	189(150,220)	<0.001
Hepatic fat, % [a]	8.0(4.4,16.5)	12.5(8.3,21.9)	15.8(9.9,25.4)	<0.001
Hepatic iron, /s [a]	44.5(37.6,55.2)	52.2(45.3,58.5)	55.4(49.6,59.3)	<0.001
Pancreatic fat, % [a]	7.0(4.2,10.5)	7.7(4.7,12.3)	12.8(7.0,18.5)	<0.001
Pancreatic iron, /s [a]	28.2(24.7,32.3)	28.5(25.9,35.4)	33.6(28.4,39.9)	<0.001

Notes: [a] Median (Q1, Q3), *b* n (%), [c] $\bar{x} \pm s$.

Abbreviations: NGR, normal glucose regulation; T2DM, type 2 diabetes mellitus; BMI, body mass index; TC, total cholesterol; TyG index, triglyceride–glucose index; HOMA-IR, homeostasis model assessment of insulin resistance; HOMA-β, homeostasis model assessment of beta-cell function; ISI, insulin sensitivity index; SFA, subcutaneous fat area; VFA, visceral fat area.

with obesity [OR = 1.11, 95% confidence interval (CI): 1.02–1.21] in the multivariable-adjusted model (Supplementary Table 3).

Changes in Regional Fat Mobilization and Organ-Specific Iron Deposition After Intervention

After a 6-month lifestyle intervention, significant reductions in weight, BMI, WHR, TG, TC, ferritin, and the TyG index were detected in obese individuals (all P<0.05). Glycemic status improved markedly: the number of T2DM patients decreased to 22, the IGR decreased to 4, and the NGR increased to 78. Concurrently, HOMA-IR decreased, whereas HOMA-β and ISI increased significantly (all P<0.05; Table 2).

After a 6-month lifestyle intervention, MRI revealed significant reductions in the SFA, VFA, hepatic fat, pancreatic fat, and hepatic and pancreatic iron contents in individuals with obesity (all P < 0.05, Supplementary Table 3). The hepatic fat content decreased the most (median reduction: 42.9% [IQR 32.4–52.4%]), followed by the pancreatic fat content (34.1% [20.0–43.1%]), VFA (19.5% [10.2–28.9%]), and SFA (12.7% [5.4–16.1%]) (P < 0.001). Moreover, the reduction in hepatic iron deposition was greater than that in pancreatic iron deposition in obese individuals (P < 0.05; Supplementary Figure 1A). Representative MR images are shown in Supplementary Figures 1B–F.

Pearson correlation analyses were conducted between site-specific reductions in adipose tissue (ΔVFA%, ΔSFA%, Δhepatic fat%, and Δpancreatic fat%), improvements in organ iron deposition (Δhepatic iron% and Δpancreatic iron%) and changes in glycemic markers (ΔHOMA-IR%, ΔISI%, and ΔHOMA-β%). The results revealed that the changes in hepatic fat content (Δhepatic fat%) and hepatic iron deposition (Δhepatic iron%) were positively correlated with ΔHOMA-IR% (insulin resistance) but negatively correlated with ΔISI% (insulin sensitivity) (all P < 0.05) in obese individuals. Conversely, the changes in pancreatic fat content (Δpancreatic fat%) and pancreatic iron deposition

Table 2 Changes in the Clinical Characteristics of Individuals with Obesity After Intervention

	Baseline (n=104)	Follow-Up (n=104)	*P* Value
Weight, kg [a]	81.6 (78.9, 89.0)	75.0 (73.7, 81.1)	<0.001
Body Mass Index, kg/m^2 [a]	31.0 (29.0, 33.2)	28.3 (27.2, 30.5)	<0.001
Waist-to-hip ratio [b]	0.95 ± 0.08	0.90 ± 0.06	<0.001
Triglycerides, mmol/L [a]	2.0 (1.2, 2.7)	1.4 (1.0, 2.3)	<0.001
Total Cholesterol, mmol/L [a]	5.2 (4.6, 5.6)	4.6 (4.1, 5.2)	<0.001
Ferritin, μg/L [a]	160 (71, 291)	112 (58, 202)	<0.001
Triglyceride index [b]	4.1±0.5	3.7 ±0.3	<0.001
Type 2 diabetes mellitus [c]	40 (38.5)	22 (21.2)	<0.001
Prediabetes [c]	23 (22.1)	4 (3.8)	<0.001
NGR [c]	41 (39.4)	78 (75.0)	<0.001
HOMA-IR [a]	5.0 (3.9, 7.2)	3.5 (2.6, 5.2)	<0.001
HOMA-β, % [a]	173 (82, 272)	198 (92, 310)	0.006
ISI [a]	32.6 (20.0, 50.2)	41.7 (26.3, 63.9)	0.020
HbA1c, % [a]	6.1 (5.9, 7.1)	5.6 (4.7, 6.2)	0.004
SFA, cm^2 [a]	221 (170, 300)	193 (161, 252)	<0.001
VFA, cm [a]	150 (107, 198)	121 (96, 141)	<0.001
Hepatic PDFF, % [a]	11.9 (6.8, 21.2)	6.8 (4.6, 10.1)	<0.001
Pancreatic PDFF, % [a]	8.8 (5.0, 14.4)	5.8 (4.0, 8.2)	<0.001
Hepatic R2*, /s [a]	50.6 (44.1, 58.8)	41.1 (36.8, 47.3)	<0.001
Pancreatic R2*, /s [a]	30.4 (25.1, 34.3)	25.3 (22.9, 29.8)	<0.001

Notes: R2*, iron deposition value. [a] Median (Q1, Q3), [b] $\bar{x} \pm s$, [c] n(%).
Abbreviations: NGR, normal glucose regulation; HOMA-IR, homeostasis model assessment of insulin resistance; HOMA-β, homeostasis model assessment of beta cell function; ISI, insulin sensitivity index. SFA, subcutaneous fat area; VFA, visceral fat area; PDFF, proton density fat fraction.

https://doi.org/10.2147/DMSO.S564591

(Δpancreatic iron%) were negatively correlated with ΔHOMA-β% (β-cell function) in individuals with obesity ($P < 0.05$, Supplementary Table 4).

Markers of Remission in Diabetes and Prediabetes Among Individuals with Obesity

Binary multivariable logistic regression was employed to assess the independent associations of potential indicators with two distinct binary outcomes: diabetes remission and the reversal of prediabetes to normal glucose regulation. For continuous variables with potential prognostic value, optimal cutoffs were determined via ROC curve analysis, and these continuous variables were dichotomized on the basis of their respective optimal cutoffs. The optimal cutoffs for reflecting T2DM remission were as follows: Δweight% ≥7.0%, ΔBMI% ≥6.5%, ΔWHR% ≥5.5%, ΔVFA% ≥20.3%, Δhepatic fat% ≥38.8%, Δhepatic iron% ≥17.4%, Δpancreatic fat% ≥28.2%, Δpancreatic iron% ≥15.0%, and ΔSFA% ≥9.2%. For reflecting the reversal of prediabetes to NGR, the optimal cutoffs were Δweight% ≥5.5%, ΔBMI% ≥5.0%, ΔWHR% ≥5.0%, ΔVFA% ≥15.5%, Δhepatic fat% ≥30.0%, Δhepatic iron% ≥15.0%, Δpancreatic fat% ≥25.5%, Δpancreatic iron% ≥10.2%, and ΔSFA% ≥7.4%.

The results indicated that in the multivariable-adjusted model, none of the variables were confirmed as independent risk factors for prediabetes remission, whereas only a Δhepatic fat% ≥38.8% was identified as an independent indicator for T2DM remission (OR = 2.50, 95% CI: 1.59–5.60) (Table 3).

We then constructed ROC curves for reflecting the remission of T2DM in individuals with obesity on the basis of BMI reduction and fat mobilization in different body regions. The areas under the ROC curve (AUCs) and 95% CIs for the percentage changes in liver fat, visceral fat, pancreatic fat, liver iron, pancreatic iron, BMI, and subcutaneous fat were 0.819 (95% CI: 0.681–0.957), 0.724 (95% CI: 0.564–0.884), 0.647 (95% CI: 0.492–0.803), 0.628 (95% CI: 0.472–0.785), 0.588 (95% CI: 0.421–0.756), 0.552 (95% CI: 0.380–0.724), and 0.547 (95% CI: 0.372–0.721), respectively (Figure 3). These results further demonstrate that the proportional reduction in liver fat is a strong indicator of T2DM remission.

Discussion

Lifestyle intervention is the first-line treatment for managing obesity. Previous studies have confirmed the effects of lifestyle intervention on the mobilization of fat from different body regions in obese individuals, as well as its role in remission of diabetes or prediabetes.[21–24] This study innovatively found that, in addition to mobilizing fat from various body regions, lifestyle intervention also led to a certain degree of improvement in hepatic and pancreatic iron load. While

Table 3 Binary Logistic Regression with Multivariable Adjustment Was Used to Assess Indicators for Diabetes Remission and the Reversal of Prediabetes

Indicators	Prediabetes Remission		Indicators	T2DM Remission	
	OR (95% CI)	*P* Value		OR (95% CI)	*P* Value
Δweight%	1.08 (0.86, 2.08)	0.572	**Δweight%**	1.02 (0.66, 2.34)	0.620
ΔBMI%	1.18 (0.69, 2.70)	0.489	**ΔBMI%**	1.08 (0.71, 2.01)	0.548
ΔWHR%	1.22 (0.74, 2.84)	0.299	**ΔWHR%**	1.10 (0.92, 3.82)	0.381
Δhepatic fat%	1.30 (0.94, 3.99)	0.145	**Δhepatic fat%**	2.50 (1.59, 5.60)	0.002*
Δhepatic iron%	1.22 (0.84, 2.57)	0.358	**Δhepatic iron%**	1.07 (0.70, 1.75)	0.402
Δpancreatic fat%	1.01 (0.98, 1.19)	0.950	**Δpancreatic fat%**	1.02 (0.73, 2.43)	0.572
Δpancreatic iron %	1.02 (0.89, 1.40)	0.914	**Δpancreatic iron %**	1.17 (0.50, 1.92)	0.797
ΔVFA%	1.19 (0.91, 3.11)	0.206	**ΔVFA%**	1.74 (0.71, 4.29)	0.592
ΔSFA%	0.84 (0.65, 1.78)	0.757	**ΔSFA%**	1.03 (0.75, 3.84)	0.330

Notes: The optimal cutoffs for reflecting T2DM remission were as follows: Δweight% ≥7.0%, ΔBMI% ≥6.5%, ΔWHR% ≥5.5%, ΔVFA% ≥20.3%, Δhepatic fat% ≥38.8%, Δhepatic iron% ≥17.4%, Δpancreatic fat% ≥28.2%, Δpancreatic iron% ≥15.0%, and ΔSFA% ≥9.2%. For reflecting the transition from prediabetes to NGR, the optimal cutoffs were Δweight% ≥5.5%, ΔBMI% ≥5.0%, ΔWHR% ≥5.0%, ΔVFA% ≥15.5%, Δhepatic fat% ≥30.0%, Δhepatic iron% ≥15.0%, Δpancreatic fat% ≥25.5%, Δpancreatic iron% ≥10.2%, and ΔSFA% ≥7.4%. * P <0.05.

Abbreviations: BMI, body mass index; WHR, waist–to–hip ratio; SFA, subcutaneous fat area; VFA, visceral fat area.

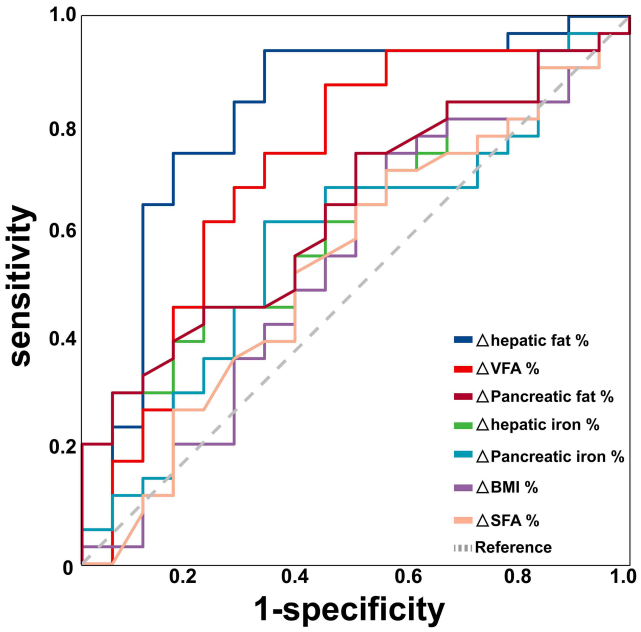

Figure 3 ROC curves reflecting the remission of type 2 diabetes in obese individuals on the basis of BMI reduction and fat mobilization in different body regions.

previous studies have demonstrated an association between hepatic iron deposition and abnormal glucose metabolism,[25,26] our longitudinal cohort study provides the first evidence that the reduction in hepatic and pancreatic iron load plays a certain role in improving insulin resistance and insulin sensitivity in individuals with obesity after lifestyle intervention. Furthermore, by incorporating hepatic fat, pancreatic fat, visceral fat, and subcutaneous fat into the same research model, we found that hepatic fat deposition has a greater impact on diabetes in obese individuals (OR=1.11, 95% CI: 1.02–1.21) than pancreatic fat (OR=0.99, 95% CI: 0.88–1.12), and even more so than visceral fat (OR=1.00, 95% CI: 0.99–1.01). Compared to fat mobilization from other regions, we found that the degree of hepatic fat mobilization was most strongly associated with the remission of T2DM in individuals with obesity (OR=2.50, 95% CI: 1.59–5.60) after lifestyle intervention. Our study also validated previous findings: when both hepatic fat and visceral fat were included simultaneously, liver fat was more strongly associated with metabolic disease progression (OR=2.7, 95% CI: 2.3–4.9) than was visceral fat (OR=2.0, 95% CI: 1.2–2.8),[27] whereas the resolution of fatty liver reduced the T2DM incidence.[28–30] The potential mechanism may be related to visceral fat driving systemic inflammation, while liver fat directly regulates glucose metabolism. Hepatic fat accumulation promotes hepatic insulin resistance and increases hepatic glucose output.[31–33] Therefore, for obese patients, prioritizing interventions targeting liver fat during weight loss may be more effective for improving diabetes. The findings of the present study indicate that lifestyle interventions (a caloric–restricted balanced diet combined with exercise) are effective approaches for preferentially mobilizing liver fat [intra-hepatic (–42.9%), pancreatic fat (–34.1%), VAT (–19.5%), and SAT (–12.7%)]. Although both the CENTRAL[34] and DiRECT[35] trials targeted multiple fat depots, hepatic fat exhibited a more marked decline than did VAT (−29% vs −22%) in the former, and hepatic fat decreased more substantially than did pancreatic fat (13% ± 1% vs 0.9% ± 0.2%) in the latter. These findings provide a rationale for future pharmacological strategies that selectively reduce liver fat to prevent or treat diabetes.

The findings of the present study revealed the differential roles of hepatic fat across different stages of glucose metabolism in individuals with obesity. In the diabetic stage, hepatic fat serves as both an independent risk factor and an indicator of remission, which corroborates the following mechanistic pathway:[36] hepatic fat accumulation → hepatic insulin resistance → increased hepatic glucose output → compensatory hyperfunction of pancreatic β-cells → development of diabetes. Conversely, a reduction in hepatic fat can improve hepatic insulin sensitivity, thereby facilitating diabetes reversal. Our study also revealed that among individuals with prediabetes, 91.3% returned to normal glucose metabolism after a 6-month lifestyle intervention. However, in the prediabetic stage, hepatic fat did not emerge as an

https://doi.org/10.2147/DMSO.S564591

independent risk factor or an indicator of remission. This may reflect a buffering effect during the compensatory phase: in individuals with prediabetes, pancreatic islet function remains relatively preserved, and compensatory hyperinsulinemia may temporarily counteract the metabolic harm caused by hepatic fat. Long-term follow-up may be needed to uncover the delayed protective effect of hepatic fat reduction in individuals who transition from prediabetes to normoglycemia. Similarly, the Tübingen Lifestyle Intervention Program (TULIP)[21] reported that the reversal of prediabetes to NGR was unrelated to adjusted body fat loss but was associated with a high-risk phenotype at baseline, defined as low insulin sensitivity (below the cohort median) combined with increased liver fat (1H-MRS with a strict threshold of >5.56% liver fat). Following this classification, we also stratified prediabetic individuals into high-risk (those with low insulin sensitivity: ISI < median + liver fat >5.56%) and low-risk phenotypes at baseline. However, after 6 months of follow-up, we did not observe significant differences in the rate of prediabetes reversal to NGR between the two groups. This discrepancy may be attributed to interethnic variability. Future studies should employ more refined phenotypic stratification and identify core regulatory targets to elucidate the heterogeneity in prediabetes intervention outcomes and optimize risk prediction models.

Hepatic lipid overflow to pancreatic tissue under chronic saturated fatty acid exposure impairs β-cell function.[37–39] While our study confirmed that higher pancreatic fat content was correlated with worse β-cell function and elevated glucose levels, it was not associated with HOMA-IR or ISI. After 6 months of lifestyle intervention, pancreatic fat mobilization (Δpancreatic fat%) correlated solely with β-cell improvement (ΔHOMA-β%), independent of insulin resistance changes, which aligns with prior evidence that pancreatic fat disrupts glucose metabolism primarily via β-cell dysfunction rather than insulin resistance.[38] Notably, although univariate analysis linked pancreatic fat reduction to glycemia remission, this association became nonsignificant after multivariable adjustment. Similarly, a 706-subject cohort revealed no independent metabolic benefit from pancreatic fat reduction,[13] suggesting that its effects may be secondary to hepatic fat mobilization. These findings further underscore the critical importance of targeting hepatic fat for glycemic improvement.

The liver, as a vital organ for iron metabolism in the body, can suffer damage due to iron overload through the induction of oxidative stress and promotion of intracellular lipid peroxidation, leading to hepatic fibrosis and cirrhosis.[40] Our present study revealed that iron deposition in both the liver and pancreas was closely associated with fat deposition. Additionally, hepatic iron deposition was significantly correlated with glucose metabolism indicators, showing a positive correlation with the insulin resistance index (HOMA-IR) and a negative correlation with the insulin sensitivity index. However, the relationship between hepatic iron deposition and these glucose metabolism indicators disappeared in the multivariate-adjusted logistic model, possibly due to collinearity between hepatic fat deposition and hepatic iron deposition. The TREND study,[41] which included 1746 German adults, revealed that hepatic iron overload was significantly positively correlated with 2-hour OGTT glucose levels. After adjusting for confounding factors, individuals with isolated hepatic iron overload showed no significant differences in fasting glucose, 2-hour glucose, or insulin levels or HOMA-IR scores, whereas those with both hepatic steatosis and iron overload presented significantly greater values of these indicators. However, as a cross-sectional study, TREND38 could not establish the causal impact of dynamic changes in hepatic iron or fat deposition on glucose metabolism. Our present study revealed that hepatic and pancreatic iron deposition significantly decreased after a 6-month lifestyle intervention, with the reduction in hepatic iron deposition showing a significant positive correlation with the decrease in HOMA-IR and a significant negative correlation with the decrease in the insulin sensitivity index. Therefore, in patients with obesity, hepatic steatosis and iron overload jointly exacerbate metabolic risk (eg, through fat-induced inflammation and iron toxicity).[25,26] For individuals with combined hepatic steatosis and iron deposition, lifestyle interventions (diet + exercise) may be more effective than iron chelation therapy. Obese individuals with iron overload should be monitored for dynamic changes in OGTTs to mitigate the risk of diabetes progression. This study has some limitations, such as a small sample size and the absence of a control group of lifestyle intervention. Future research incorporating randomized controlled designs would help validate these findings.

Our findings underscore the clinical importance of liver fat assessment in obesity management, while simultaneously highlighting practical challenges in implementing MRI-based quantification in routine practice. Although MRI-PDFF remains the gold standard for hepatic fat quantification, its widespread clinical adoption faces significant barriers including time-intensive manual analysis, the need for specialized radiological expertise, and limited availability of advanced 3T MRI

systems with appropriate sequences in many clinical settings. In light of these technical limitations, several practical approaches have emerged for real-world monitoring: risk-stratified MRI utilization prioritizing high-risk patients with combined steatosis and iron overload, surrogate biomarkers incorporating FibroScan measurements and ALT trends for resource-limited settings. Particularly promising are recent advances in AI-assisted quantification which have achieved 0.99 correlation with manual segmentation while reducing analysis time to under 2 minutes per case.[42] For clinical implementation, we propose a tiered monitoring framework beginning with comprehensive baseline MRI assessment, followed by quarterly biomarker surveillance (ALT, ferritin) and annual FibroScan evaluations for stable patients, reserving repeat MRI for cases showing significant metabolic changes. This approach strategically balances precision with practicality, addressing the critical translational challenge of implementing hepatic fat monitoring across diverse healthcare settings. While these technological advancements in automated analysis are enhancing MRI's scalability, further cost-effectiveness analyses remain necessary to guide widespread adoption in routine obesity management protocols.

In conclusion, dynamic changes in hepatic fat deposition (accumulation and mobilization) represent key pathophysiological mechanisms underlying both the development and remission of dysglycemia in individuals with obesity. Our findings demonstrate that targeted interventions addressing hepatic steatosis can effectively ameliorate obesity-related metabolic dysfunction. Specifically, hepatic fat quantification should be incorporated into routine metabolic risk stratification for obese individuals, particularly those with T2DM. Therapeutic strategies should prioritize liver-specific fat reduction through structured lifestyle interventions combining moderate caloric restriction (−500 kcal/day) and supervised exercise (≥150 min/week). Future multi-center research should validate these thresholds across diverse populations while developing cost-effective monitoring protocols, such as rapid MRI techniques, for widespread clinical implementation.

Data Sharing Statement

The data supporting the findings of this study are available within the article and its supplementary materials.

Ethics Approval and Informed Consent

This study complies with the Declaration of Helsinki. All study subjects signed an informed consent form. Ethical approval was granted by the Ethics Committee of The Third Xiangya Hospital of Central South University (approval number I 22218) and registered at ClinicalTrials.gov (No. NCT06441409).

Consent for Publication

We affirm that the specifics of any images, videos, recordings, etc, are authorized for publication, and the individuals granting consent have been informed about the content of the article that will be published.

Acknowledgments

We would like to thank all the participants in this study for their cooperation. We also acknowledge the efforts of our nutritionists Ms. Min Liu and Ms. Yufang Luo for following up with patients.

Author Contributions

Hong Liu: Data curation (equal); formal analysis (equal); investigation (equal); project administration (equal); writing – original draft (lead). Junhong Duan: Data curation (equal); formal analysis (equal); project administration (equal). Gaopeng Guan: Data curation (equal); project administration (equal). Pengfei Rong: Data curation (equal); formal analysis (equal). Ping Jin: Data curation (equal); formal analysis (equal); investigation (equal); project administration (equal); writing – review and editing (equal). All authors took part in drafting, revising or critically reviewing the article; gave final approval of the version to be published; have agreed on the journal to which the article has been submitted; and agree to be accountable for all aspects of the work.

Funding

This study was supported by the Natural Science Foundation of Hunan Province, China (2024JJ9052, 2022JJ40749).

Disclosure

The author(s) report no conflicts of interest in this work.

References

1. NCD Risk Factor Collaboration (NCD-RisC). Worldwide trends in underweight and obesity from 1990 to 2022: a pooled analysis of 3663 population-representative studies with 222 million children, adolescents, and adults. *Lancet*. 2024;403(10431):1027–1050. doi:10.1016/S0140-6736(23)02750-2
2. Jamjl J. The causal role of ectopic fat deposition in the pathogenesis of metabolic syndrome. *Int J Mol Sci*. 2024;25(24):13238. doi:10.3390/ijms252413238
3. Cao MJ, Wu WJ, Chen JW, et al. Quantification of ectopic fat storage in the liver and pancreas using six-point Dixon MRI and its association with insulin sensitivity and β-cell function in patients with central obesity. *Eur Radiol*. 2023;33(12):9213–9222. doi:10.1007/s00330-023-09856-x
4. Mk S, Saucedo A, Darwin CH, et al. Noninvasive assessment of abdominal adipose tissues and quantification of hepatic and pancreatic fat fractions in type 2 diabetes mellitus. *Magn Reson Imaging*. 2020;72:95–102. doi:10.1016/j.mri.2020.07.001
5. Gao H, Yang J, Pan W, et al. Iron overload and the risk of diabetes in the general population: results of the Chinese Health and Nutrition Survey Cohort Study. *Diabetes Metab J*. 2022;46(2):307–318. doi:10.4093/dmj.2020.0287
6. Liu J, Li Q, Yang Y, et al. Iron metabolism and type 2 diabetes mellitus: a meta-analysis and systematic review. *J Diabetes Investig*. 2020;11(4):946–955. doi:10.1111/jdi.13216
7. Naim M, Amal A, Zeynep K, et al. Ferritin - from iron, through inflammation and autoimmunity, to COVID-19. *J Autoimmun*. 2022;126:102778. doi:10.1016/j.jaut.2021.102778
8. Moreira AC, Mesquita G, Gomes MS. Ferritin: an Inflammatory player keeping iron at the core of pathogen interactions. *Microorganisms*. 2020;8(4):589. doi:10.3390/microorganisms8040589
9. Brzezinski RY, Wasserman A, Sasson N, et al. An exploratory analysis of routine ferritin measurement upon admission and the prognostic implications of low-grade ferritinemia during inflammation. *Am J Med*. 2024;137(9):865–871.e1. doi:10.1016/j.amjmed.2024.04.033
10. Kim JW, Lee CH, Yang Z, et al. The spectrum of magnetic resonance imaging proton density fat fraction (MRI-PDFF), magnetic resonance spectroscopy (MRS), and two different histopathologic methods (artificial intelligence vs. pathologist) in quantifying hepatic steatosis. *Quant Imaging Med Surg*. 2022;12(11):5251–5262. doi:10.21037/qims-22-393
11. Karolina G, Michał G, Olgierd R. Usefulness of different imaging modalities in evaluation of patients with non-alcoholic fatty liver disease. *Biomedicines*. 2020;8(9):298. doi:10.3390/biomedicines8090298
12. London A, Lundsgaard A, Kiens B, et al. The role of hepatic fat accumulation in glucose and insulin homeostasis-dysregulation by the liver. *J Clin Med*. 2021;10(3):390. doi:10.3390/jcm10030390
13. Deng M, Li Z, Chen SY, et al. Exploring the heterogeneity of hepatic and pancreatic fat deposition in obesity: implications for metabolic health. *Front Endocrinol*. 2024;8:1447750. doi:10.3389/fendo.2024.1447750
14. Eckard C, Cole R, Lockwood J, et al. Prospective histopathologic evaluation of lifestyle modification in nonalcoholic fatty liver disease: a randomized trial. *Therap Adv Gastroenterol*. 2013;6(4):249–259. doi:10.1177/1756283X13484078
15. Mascaró CM, Bouzas C, Montemayor S, et al. Effect of a six-month lifestyle intervention on the physical activity and fitness status of adults with NAFLD and metabolic syndrome. *Nutrients*. 2022;14(9):1813. doi:10.3390/nu14091813
16. Walden P, Jiang Q, Jackson EA, et al. Assessing the incremental benefit of an extended duration lifestyle intervention for the components of the metabolic syndrome. *Diabetes Metab Syndr Obes*. 2016;9:177–184. doi:10.2147/DMSO.S94772
17. Saha S, Leijon M, Gerdtham U, et al. A culturally adapted lifestyle intervention addressing a Middle Eastern immigrant population at risk of diabetes, the MEDIM (impact of Migration and Ethnicity on Diabetes In Malmö): study protocol for a randomized controlled trial. *Trials*. 2013;14:279. doi:10.1186/1745-6215-14-279
18. Hopewell S, Chan AW, Collins GS, et al. CONSORT 2025 statement: updated guideline for reporting randomised trials.*BMJ*. 2025; 389: e081123.
19. Fpb K, Dh C, Callaghan BC, et al. The prevalence of polyneuropathy in type 2 diabetes subgroups based on HOMA2 indices of β-cell function and insulin sensitivity. *Diabetes Care*. 2023;46(8):1546–1555. doi:10.2337/dc23-0079
20. Brunt EM, Janney CG, AMDi B, et al. Nonalcoholic steatohepatitis: a proposal for grading and staging the histological lesions. *Am J Gastroenterol*. 1999;94(9):2467–2474. doi:10.1111/j.1572-0241.1999.01377.x
21. Stefan N, Staiger H, Wagner R, et al. A high-risk phenotype associates with reduced improvement in glycemia during a lifestyle intervention in prediabetes. *Diabetologia*. 2015;58(12):2877–2884. doi:10.1007/s00125-015-3760-z
22. Kabisch S, Meyer NMT, Honsek C, et al. Predicting factors for metabolic non-response to a complex lifestyle intervention-A replication analysis to a randomized-controlled trial. *Nutrients*. 2022;14(22):4721. doi:10.3390/nu14224721
23. Grune E, Nattenmüller J, Kiefer LS, et al. Subphenotypes of body composition and their association with cardiometabolic risk – magnetic resonance imaging in a population-based sample. *Metabolism*. 2025;164:156130. doi:10.1016/j.metabol.2024.156130
24. Linge J, Borga M, West J, et al. Body composition profiling in the UK Biobank imaging study. *Obesity*. 2018;26(11):1785–1795. doi:10.1002/oby.22210
25. Pitchika A, Kühn JP, Schipf S, et al. Hepatic steatosis and hepatic iron overload modify the association of iron markers with glucose metabolism disorders and metabolic syndrome. *Liver Int*. 2021;41(8):1841–1852. doi:10.1111/liv.14868
26. Niedermayer F, Su YQ, Krüchten RV, et al. Trajectories of glycemic traits exhibit sex-specific associations with hepatic iron and fat content: results from the KORA-MRI study. *Liver Int*. 2023;43(10):2153–2166. doi:10.1111/liv.15635
27. Basheer M, Saad E, Jeries H, et al. Liver fat storage is a better predictor of coronary artery disease than visceral fat. *Metabolites*. 2023;13(8):896. doi:10.3390/metabo13080896
28. Yang M, Chen J, Yue J, et al. Liver fat is superior to visceral and pancreatic fat as a risk biomarker of impaired glucose regulation in overweight/obese subjects. *Diabetes Obes Metab*. 2023;25(3):716–725. doi:10.1111/dom.14918
29. Fukuda T, Hamaguchi M, Kojima T, et al. Transient remission of nonalcoholic fatty liver disease decreases the risk of incident type 2 diabetes mellitus in Japanese men. *Eur J Gastroenterol Hepatol*. 2016;28(12):1443–1449. doi:10.1097/MEG.0000000000000736

30. Chen CL, Zhang YC, Fan YJ, et al. The change of nonalcoholic fatty liver disease is associated with risk of incident diabetes. *Front Endocrinol*. 2023;14:1108442. doi:10.3389/fendo.2023.1108442
31. Fan ZX, Yang CJ, Zhao XJ, et al. Association of cardiometabolic markers with hepatic steatosis and liver fibrosis in population without obesity and diabetes. *Sci Rep*. 2025;15(1):15695. doi:10.1038/s41598-025-01003-4
32. Gangireddy VGR, Pilkerton C, Xiang J, et al. Hepatic fibrosis and steatosis in metabolic syndrome. *J Obes Metab Syndr*. 2022;31(1):61–69. doi:10.7570/jomes21062
33. Liang ZT, Huang RH, Zhang LY. Correlation between hepatic steatosis severity diagnosed by ultrasound and metabolic indices in elderly patients with MAFLD. *Front Med Lausanne*. 2025;11:1467773. doi:10.3389/fmed.2024.1467773
34. Gepner Y, Shelef I, Schwarzfuchs D, et al. Effect of distinct lifestyle interventions on mobilization of fat storage pools: CENTRAL magnetic resonance imaging randomized controlled trial. *Circulation*. 2018;137(11):1143–1157. doi:10.1161/CIRCULATIONAHA.117.030501
35. Taylor R, Leslie WS, Barnes AC, et al. Clinical and metabolic features of the randomized controlled diabetes remission clinical trial (DiRECT) cohort. *Diabetologia*. 2018;61(3):589–598. doi:10.1007/s00125-017-4503-0
36. Taylor R, Al-Mrabeh A, Sattar N. Understanding the mechanisms of reversal of type 2 diabetes. *Lancet Diabetes Endocrinol*. 2019;7(9):726–736. doi:10.1016/S2213-8587(19)30076-2
37. Al-Mrabeh A, Zhyzhneuskaya SV, Peters C, et al. Hepatic lipoprotein export and remission of human type 2 diabetes after weight loss. *Cell Metab*. 2020;31(2):233–249.e4. doi:10.1016/j.cmet.2019.11.018
38. Wu WJ. Diabetes remission and nonalcoholic fatty pancreas disease. *World J Diabetes*. 2024;15(7):1390–1393. doi:10.4239/wjd.v15.i7.1390
39. Wagner R, Eckstein SS, Yamazaki H, et al. Metabolic implications of pancreatic fat accumulation. *Nat Rev Endocrinol*. 2022;18(1):43–54. doi:10.1038/s41574-021-00573-3
40. Anderson ER, Shah YM. Iron homeostasis in the liver. *Compr Physiol*. 2013;3(1):315–330. doi:10.1002/j.2040-4603.2013.tb00494.x
41. Naeem M, Schipf S, Bülow R, et al. Association between hepatic iron overload assessed by magnetic resonance imaging and glucose intolerance states in the general population. *Nutr Metab Cardiovasc Dis*. 2022;32(6):1470–1476. doi:10.1016/j.numecd.2022.02.013
42. Wei JY, Chen HL, Yao LJR, et al. BioCompNet: a deep learning workflow enabling automated body composition analysis toward precision management of cardiometabolic disorders. *Cyborg Bionic Syst*. 2025;20:381. doi:10.34133/cbsystems.0381